Geophysical Research Letters

RESEARCH LETTER
10.1029/2024GL113037

Key Points:

- Singapore Airlines flight SQ321 encountered severe turbulence in an area where developing convection was present
- ECMWF IFS was able to predict the occurrence of convection and associated convectively induced turbulence more than 24 hr in advance
- Probabilities from ensemble forecasts must be taken with care when convection is involved because of the variability in time and space

Supporting Information:

Supporting Information may be found in the online version of this article.

Correspondence to:

S. Gisinger,
sonja.gisinger@dlr.de

Citation:

Gisinger, S., Bramberger, M., Dörnbrack, A., & Bechtold, P. (2024). Severe convectively induced turbulence hitting a passenger aircraft and its forecast by the ECMWF IFS model. *Geophysical Research Letters*, *51*, e2024GL113037. https://doi.org/10.1029/2024GL113037

Received 17 OCT 2024
Accepted 4 NOV 2024

Author Contributions:

Conceptualization: S. Gisinger, A. Dörnbrack
Formal analysis: S. Gisinger, P. Bechtold
Visualization: S. Gisinger, M. Bramberger
Writing – original draft: S. Gisinger, M. Bramberger
Writing – review & editing: M. Bramberger, A. Dörnbrack, P. Bechtold

Severe Convectively Induced Turbulence Hitting a Passenger Aircraft and Its Forecast by the ECMWF IFS Model

S. Gisinger[1], M. Bramberger[2], A. Dörnbrack[1], and P. Bechtold[3]

[1]Deutsches Zentrum für Luft- und Raumfahrt, Institut für Physik der Atmosphäre, Oberpfaffenhofen, Germany, [2]National Center for Atmospheric Research, Boulder, CO, USA, [3]European Centre for Medium-Range Weather Forecasts, Bonn, Germany

Abstract Atmospheric turbulence poses a major risk to aviation. Besides airframe damage, it can cause injuries of passengers and crew when encountered unexpectedly. The Singapore Airlines flight SQ321 was on its way from London to Singapore when severe turbulence was encountered over Myanmar on 21 May 2024. In this study, it is analyzed how well the turbulence was predicted by the turbulent eddy dissipation rate (EDR) forecast index of the ECMWF integrated forecasting system (IFS). It was found that ECMWF IFS was able to predict the convection and associated turbulence 24 hr in advance. The state-of-the-art probabilistic EDR forecasts based on IFS ensemble members predicted probabilities for EDR >0.18 $m^{2/3}$ s^{-1} between 10% and 40% over Myanmar with higher values for shorter lead time (8-hr forecast). Individual members predicted EDR >0.3 $m^{2/3}$ s^{-1}. Knowledge about the characteristics of convection in the IFS forecasts is required to make proper use of the probabilities determined from the ensemble for such cases.

Plain Language Summary Atmospheric turbulence is a threat to aircraft because it is invisible to pilots in the absence of clouds and therefore often encountered unexpectedly. Turbulence is usually found close to mountains, near the atmospheric jet streams, or thunderstorms. A severe turbulence encounter can damage the airframe and cause injuries of passengers and crew. The Singapore Airlines flight SQ321 was on its way from London to Singapore when severe turbulence was encountered over Myanmar on 21 May 2024. Abrupt rapid changes in flight altitude including a drop of 178 ft left one passenger dead and dozens injured. In this study, it was found, that the turbulence forecast of the European Centre for Medium-Range Weather Forecasts (ECMWF) was able to predict the convection in the area and the associated turbulence 24 hr in advance. However, convection cannot be exactly predicted in time and space, so knowledge about the characteristics of the forecast of convection is needed to properly interpret such turbulence forecasts.

1. Introduction

Atmospheric turbulence poses a major risk to aviation and causes significant cost to the aviation industry (Eichenbaum, 2003). In this context turbulence can cause airframe fatigue and occasional airframe damage as well as injuries of passengers and crew. Recent studies show that clear air turbulence (CAT) occurrence and magnitudes increased significantly due to changing climate making it 37% more likely to encounter moderate-or-greater turbulence compared to 1979 (Prosser et al., 2023; Williams, 2017). For the high-emission scenario (SSP5-8.5; 2056–2100), convectively induced turbulence (CIT) was found to increase over the tropics and extratropics for all seasons compared to historical values (1970–2014) (S.-H. Kim et al., 2023). The predicted increase of aviation turbulence highlights the necessity for reliable forecasts.

Despite a general trend to increase the resolution in operational forecasting models, turbulence on the scale that affects aircraft is not resolved in state-of-the-art models (R. Sharman et al., 2006; R. D. Sharman & Pearson, 2017). As grid sizes are larger than the size of turbulent eddies, operational forecasts typically use a collection of empirical turbulent indices to predict turbulence relevant to aviation (R. Sharman et al., 2006; R. D. Sharman & Pearson, 2017; J. Kim & Chun, 2012a). These indices that cover different sources for turbulence are combined to derive the cube-root of the energy dissipation rate (EDR), a common, aircraft-independent parameter to indicate the strength of turbulence (R. D. Sharman & Pearson, 2017). EDR can be translated to turbulence intensity depending on aircraft size, that is, moderate turbulence for EDR >0.18 $m^{2/3}$ s^{-1} and EDR >0.27 $m^{2/3}$ s^{-1} for light and heavy aircraft, respectively (Sharman et al., 2014).

Turbulence is usually generated by (breaking) mountain waves, shear instabilities near jet streams, or convection (R. D. Sharman et al., 2012). CIT can be separated into in-cloud CIT caused by moist instabilities and mixing near updrafts, downdrafts, and specific cloud features and out-of-cloud CIT caused by convection-induced enhanced background wind shear and convectively generated gravity waves (Barber et al., 2019; Lane et al., 2012). Avoidance of turbulence in cloudy air through visual identification or remote sensing with radar and satellite imagery is usually effective (Lane et al., 2012). Out-of-cloud CIT is also called near-cloud turbulence (NCT) and like mountain wave turbulence (MWT) and CAT invisible to pilots (Lane et al., 2012). Of these types, CIT continues to pose a challenge for forecasting models because its generation mechanism including initiation and development of convection is also not fully resolved in models and needs to be parameterized. Thus, current operational systems struggle to predict the correct time and space of convective cells further complicating CIT forecasting (Barber et al., 2019). Nevertheless, NCT diagnostics based on post processing with a convective gravity wave drag parametrization above convective cloud tops were found to improve the turbulence forecasting skill, especially in the tropics, when added to conventional CAT diagnostics (S.-H. Kim et al., 2021). As CIT can even occur in regions where onboard radar does not indicate turbulent or convective conditions (J. Kim & Chun, 2012b), the Federal Aviation Administration (FAA) has issued guidelines recommending that pilots stay 20 mi (32.2 km) away from severe convection to reduce the number of incidents (FAA, 2017).

In the present study we investigate a recent turbulence encounter by a passenger aircraft that received much attention in the public. We analyze how well the encountered turbulence in the area was predicted by the EDR index that was implemented in the European Centre for Medium-Range Weather Forecasts (ECMWF) integrated forecasting system (IFS) in recent years (Bechtold et al., 2021). Our hypothesis is that the ECMWF IFS EDR index could forecast this event 24 hr in advance and taking into account contributions by convection was crucial. This is the first investigation of such a convective turbulence event by means of operationally available state-of-the art ECMWF IFS ensemble forecast of EDR. In the following Section 2 will describe the turbulence incident, Section 3 will present details and results of the ECMWF IFS EDR index and Section 4 will conclude this study with a brief discussion and outlook.

2. Severe Turbulence Incident on 21 May 2024

The Singapore Airlines flight SQ321 was on its way from London (departure 20 May 2024 21:38 UTC) to Singapore when severe turbulence was encountered at 7:49 UTC on 21 May 2024 over Myanmar (Figure 1a). Abrupt rapid changes in flight altitude (Figure 1b) left one passenger dead and dozens injured (see Open Research Section for details). After the incident, the flight was diverted to Bangkok (Figure 1a).

2.1. Preliminary Investigation Findings of Incident

Preliminary findings by investigators of the Transport Safety Investigation Bureau of Singapore (TSIB), United States representatives, the National Transportation Safety Board (NTSB), Federal Aviation Administration (FAA) and Boeing were released on 29 May 2024 (MOT, 2024). Data stored in the flight data recorder (FDR) and cockpit voice recorder (CVR) were analyzed and lead to the following chronology and description of events (following paragraph is a summary of the report (MOT, 2024) using its original wording): At 07:49:21 UTC on 21 May 24, the aircraft was passing over the south of Myanmar at 37,000 ft and likely flying over an area of developing convective activity. The onset of the slight vibration was registered and an uncommanded increase in aircraft altitude, reaching a peak of 37,362 ft, was recorded (Figure 1b). This uncommanded increase in aircraft altitude and airspeed was most likely due to the aircraft being acted upon by an updraft. Rapid changes in the vertical acceleration over a period of 4.6 s resulted in passengers who were not belted up to first become airborne and then fell back down. During that period, an altitude drop of 178 ft, from 37,362 ft to 37,184 ft was recorded. In the midst of this sequence, recorded data indicate that the pilots initiated control inputs to stabilize the aircraft, disengaging the autopilot in this process. The pilots manually controlled the aircraft for 21 s and reengaged the autopilot at 07:50:05 UTC. The recorded vertical acceleration showed more gradual fluctuations over the next 24 s while the aircraft returned to 37,000 ft at 07:50:23 UTC. Approximately 17 min after the turbulence event, at 08:06:51 UTC, the pilots initiated a normal, controlled descent from 37,000 ft and the aircraft reached 31,000 ft at 08:10:00 UTC. The data showed that the aircraft did not encounter further severe turbulence during this diversion, and touched down in Suvarnabhumi Airport, Bangkok, at 08:45:12 UTC (MOT, 2024).

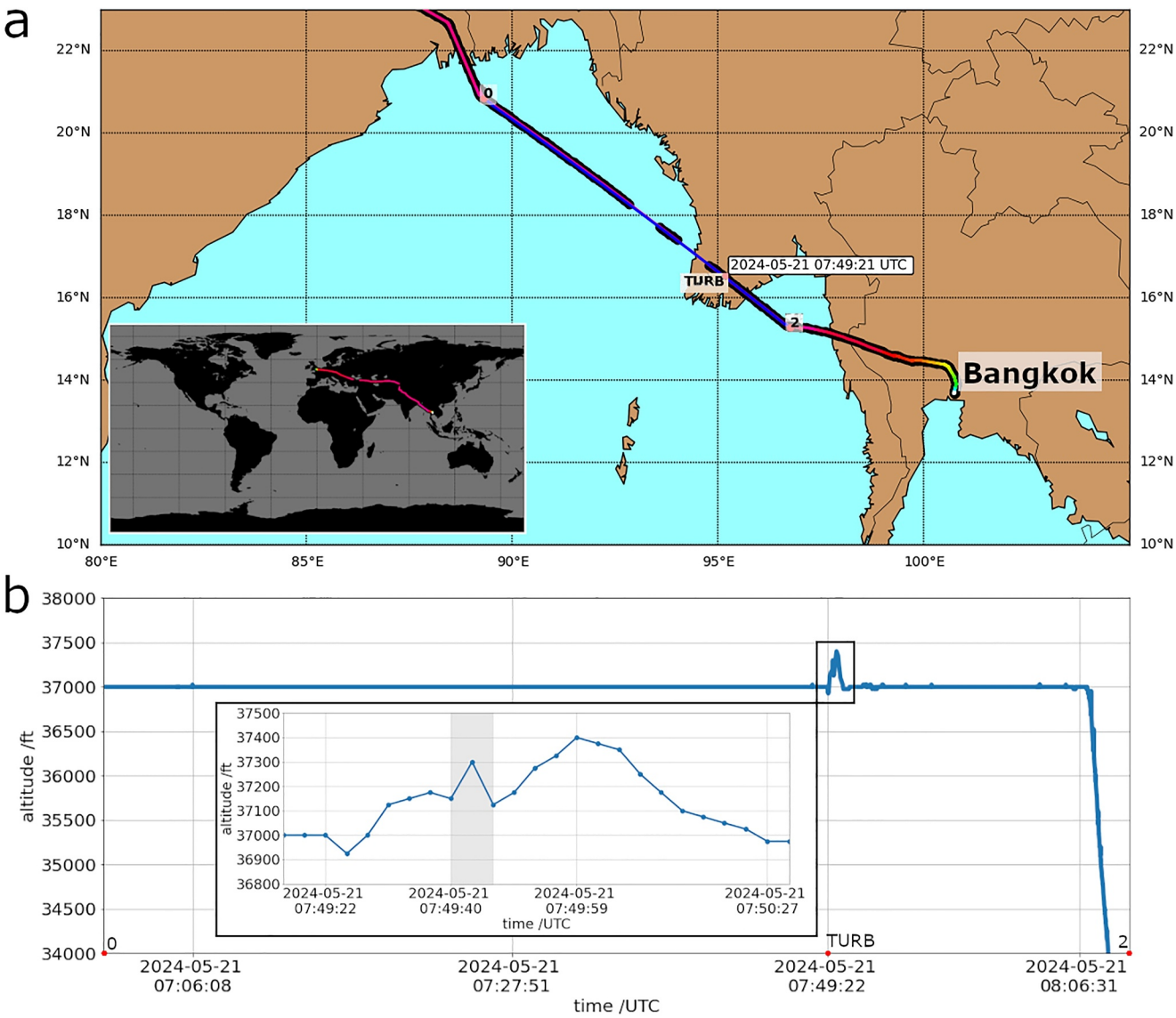

Figure 1. (a) Map showing the region where the turbulence incident occurred on 21 May 2024 at 07:49 UTC. The segment used in the Mission Support System (MSS) tool (Bauer et al., 2024) is marked by waypoint 0 and waypoint 2 with the waypoint TURB inbetween. The full flight track from London to Bangkok is shown in the lower left panel. (b) Flight altitude as reported by ADS-B data (see Open Research Section for details) and zoom of the incident. Gray shading marks the most rapid changes in vertical acceleration.

By combining the time of the uncommanded increase to maximum flight altitude, that is, 37 seconds (Figure 1b), with the mean ground speed of 257 m s^{-1} during that period, we can estimate the size of the updraft region along the flight track to be approximately 9.5 km. The average total increase in flight altitude by 362 ft (110 m) in 37 s is similar to the rate of change in altitude of 50 m in 15 s that the research aircraft HALO (High-Altitude and Long-Range Research Aircraft) experienced in a MWT encounter above Iceland in October 2016 (Bramberger et al., 2020).

2.2. Convection in the Area

On 21 May 2024, the Madden–Julian oscillation was active and in Phase 3 (AusGBM, 2024) leading to enhanced convection over the Indian Ocean (Wheeler & Hendon, 2004). The incident took place close to 8 UTC which is 15:30 local time in Myanmar when land areas are typically heated by incoming solar radiation. The presence of extensive cloud cover earlier on that day would have reduced the surface heating. The satellite image at 8 UTC

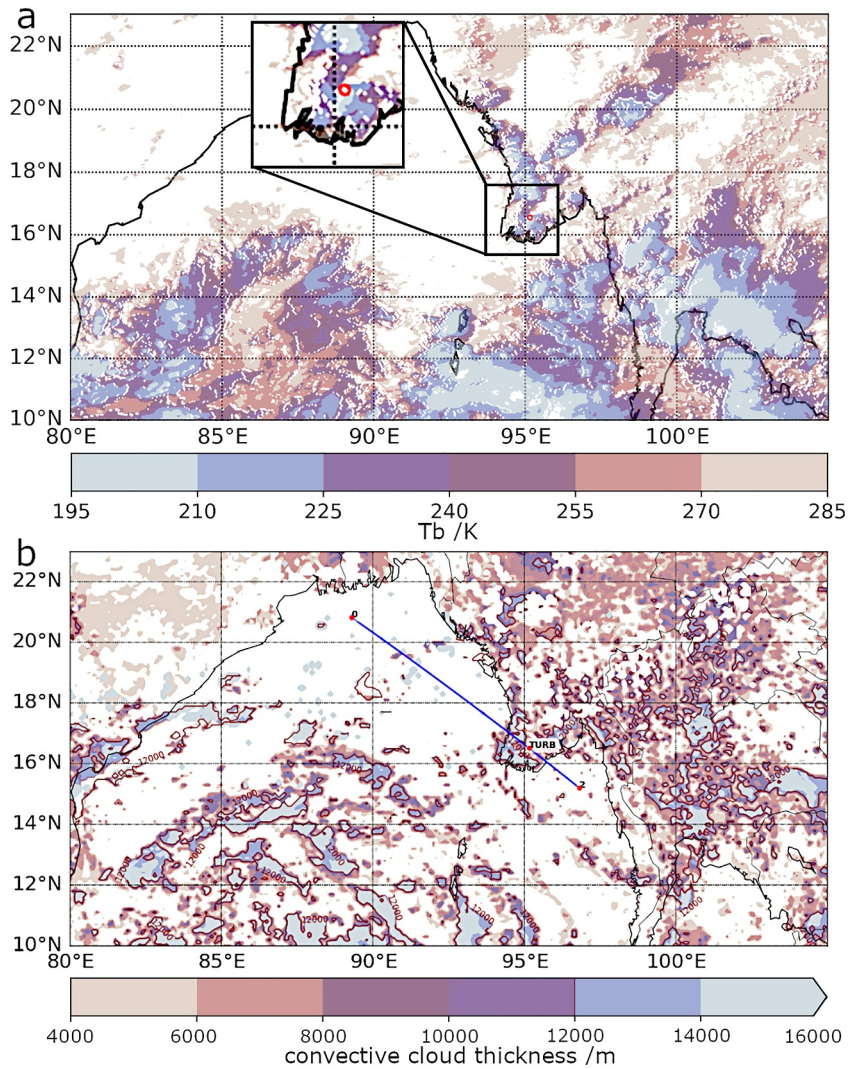

Figure 2. (a) Satellite image of Himawari-8 showing the developing convective clouds by means of brightness temperature (Tb) on 21 May 2024 08 UTC. The red circle shown at location TURB has a diameter of approximately 10 km. The insert shows a zoom to the region of the incident. (b) ECMWF IFS forecast showing the thickness of convective clouds (= height of convective cloud top by parameterized convection minus cloud base height (ECMWF, 2020)) on 21 May 2024 08 UTC visualized with the MSS tool. Heights of the convective cloud top of 12,000 m are marked by the dark red isolines. The forecast was initialized on 20 May 2024 00 UTC.

shows high (cold) convective clouds in the innertropical convergence zone (ITCZ) around 12°N (brightness temperatures of less than 210 K). Developing convection along the southern coast of Myanmar shows up by small cloud patches having low brightness temperatures (Figure 2a). At the location of the incident which is marked by a red circle of 10 km diameter (estimated size of the updraft, Sec. 2.1) in Figure 2a, the extent of the cloud patch with brightness temperature less than 210 K is approximately 10 km along flight direction and approximately 20–30 km in cross flight direction. Although it is impossible to exactly forecast convection in time and space, the ECMWF IFS forecast for 8 UTC, which was initialized at 20 May 2024 00 UTC, shows similar convective clouds in the region in Figure 2b. The thickness of convective clouds (Figure 2b) shows where the convection scheme is active and convective clouds with a depth of >4000 m are produced. In the area of the peninsula, where the incident occurred, clouds were mainly found over land but not over the ocean which suggests that the diurnal heating of the land in the course of the day triggered the convection, possibly in combination with the land-sea breeze leading to convergence in the lower troposphere (see Figure S1 in Supporting Information S1) and upward motion in the middle and upper troposphere. Height of the convective cloud top was forecasted to be 12,000 m and higher close to the incident (Figure 2b).

3. ECMWF IFS EDR Turbulence Forecast

3.1. ECMWF IFS Model Configuration

The ECMWF IFS provides global medium-range (up to 15 days) forecasts. The IFS cycle 48r1 became operational on 27 June 2023. The medium-range forecast has a horizontal grid-spacing of ≈ 9 km on the cubic octahedral grid (TCo1279). Model data were retrieved on a regular $0.1° \times 0.1°$ latitude-longitude grid. The model top is located at 0.01 hPa ($z \approx 80$ km) and 137 vertical levels are used. The layer thickness gradually increases with altitude and is ~ 300 m at $z \approx 10$ km. The IFS ensemble (ENS) consists of 50 members and one control run. The latter has the same initial conditions as the deterministic HRES (high-resolution) run. The horizontal resolution of the ENS is identical to the HRES run for cycle 48r1 (ECMWF, 2023b), so the HRES run now represents one possible realization of the future state of the atmosphere with the same likelihood of occurrence as every individual member of the ensemble.

3.2. EDR Index Based on the Total Dissipation Rate

A calibrated EDR index for the troposphere and stratosphere has been developed in the ECMWF IFS based on the idea of R. D. Sharman and Pearson (2017) to use multiple parameters. It was found that an EDR based on a modified Ellrod1 index and/or the total dissipation rate that is derived from the subgrid physical momentum tendencies of the IFS, provide useful guidance for severe turbulence (Bechtold et al., 2021). Due to archiving and computational constraints only calculation of the EDR index based on the total dissipation rate was put into operations with IFS cycle 47r3 on 12 October 2021.

The total dissipation rate (DISS) of the IFS in units of EDR is derived from the model's physical tendencies for horizontal momentum. It includes contributions from the vertical diffusion scheme, the convective momentum transport and the convective gravity wave drag (GWD)

$$\mathrm{DISS} = \left|\left(u\frac{\partial u}{\partial t}|_{\mathrm{diff}} + v\frac{\partial v}{\partial t}|_{\mathrm{diff}}\right)\right|^{1/3} + \left|\left(u\frac{\partial u}{\partial t}|_{\mathrm{conv}} + v\frac{\partial v}{\partial t}|_{\mathrm{conv}}\right)\right|^{1/3} + \mathrm{GWD}, \tag{1}$$

where

$$\mathrm{GWD} = \left[\left|\left(u\frac{\partial u}{\partial t}|_{\mathrm{gwd}} + v\frac{\partial v}{\partial t}|_{\mathrm{gwd}}\right)\right|\hat{T}_{\mathrm{conv}}\right]^{1/3}, \tag{2}$$

$$\hat{T}_{\mathrm{conv}} = -\frac{c_p}{\hat{T}_0}\int_{p=500hPa}^{top}\frac{\partial T}{\partial t}|_{\mathrm{conv}}\frac{dp}{g}. \tag{3}$$

The vertical diffusion scheme (diff) includes dissipation due to turbulent mixing (Chapter 3 in ECMWF (2023a)), orographic wave drag and orographic blocking (Chapter 4 in ECMWF (2023a)). The subscript gwd denotes the tendencies (wave drag) from the non-orographic wave scheme (Chapter 5 in ECMWF (2023a)) and the subscript conv the temperature tendency from the convection parametrization (Chapter 6 in ECMWF (2023a)), g is gravity and c_p the specific heat at constant pressure. $\hat{T}$ is normalized by $\hat{T}_0 = 1$ W m^{-2}. The EDR index for aircraft turbulence is 2/3 DISS (Bechtold et al., 2021; Dörnbrack et al., 2022) based on the calibration with commercial aircraft data (R. D. Sharman & Pearson, 2017).

This approach differs from other turbulence forecasts like the Graphical Turbulence Guidance (GTG) system, which is a post-processing of the model output of resolved quantities to determine a range of different CAT indices and the German Weather Service (DWD) CAT predictions, which are based on the subgrid-scale turbulent kinetic energy equation (Dörnbrack et al., 2022, and references therein). Direct comparison with EDR determined from research aircraft observations during SOUTHTRAC (Rapp et al., 2021) revealed the benefit of the IFS EDR ensemble forecast (Dörnbrack et al., 2022). The small fraction of moderate turbulence (EDR >0.18 m$^{2/3}$ s^{-1}) observed by HALO is not reproduced by a 15-member ensemble mean, however, investigating the individual ensemble members revealed the potential of individual ensemble members to predict enhanced turbulence (Dörnbrack et al., 2022). A statistical 3-month validation of IFS EDR forecasts against commercial aircraft data can be found in Appendix A of Dörnbrack et al. (2022). Although this validation is not restricted to convective

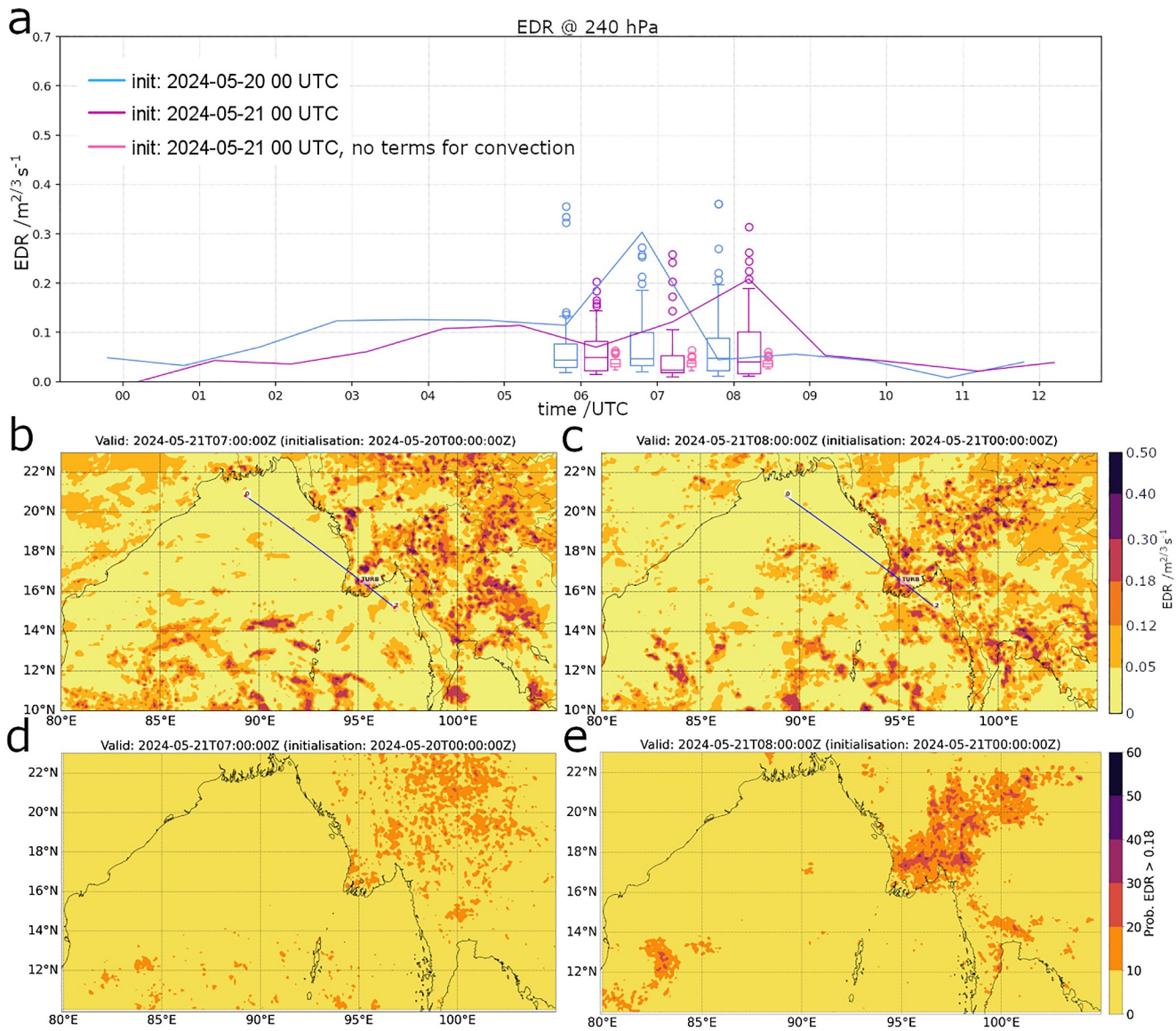

Figure 3. (a) Time series showing EDR at 240 hPa at the location of the incident (TURB) for the IFS HRES forecasts initialized on 20 May 2024 00 UTC with lead time 24–36 hr (blue) and initialized on 21 May 2024 00 UTC with lead time 0–12 hr (purple). Boxplot shows the corresponding IFS ENS (median, 10th/90th percentiles, and maximum extremes) for 06, 07, and 08 UTC including (blue, purple) and without terms for convection (pink) in Equation 1. (b) EDR ($m^{2/3}$ s^{-1}) at 240 hPa on 21 May 2024 07 UTC of the ECMWF IFS HRES forecast initialized on 20 May 2024 00 UTC (lead time 31 hr) and (c) on 21 May 2024 08 UTC of the ECMWF IFS HRES forecast initialized on 21 May 2024 00 UTC (lead time 8 hr). Maps were visualized with the MSS tool (d), (e) Corresponding probability for EDR >0.18 $m^{2/3}$ s^{-1} computed from the IFS ENS.

conditions, we want to mention here that the mean point correlations of the 15-member ensemble reach 0.37 for IFS EDR based on DISS (named CAT2 in Dörnbrack et al. (2022)) which lies between 0.53 and 0.2–0.4 obtained for 10-m wind speed forecasts over land and integrations of daily rainfall over tropical land, respectively (Dörnbrack et al., 2022). With the introduction of IFS Cycle 48r1 and the availability of a high-resolution (≈ 9 km) 51-member ensemble since June 2023, the EDR index became a fully probabilistic product of the ECMWF IFS. Ensemble predictions are inevitably required to capture the range of possible model outcomes (Lane et al., 2012).

3.3. IFS Forecast for 21 May 2024

IFS forecasts initialized on 00 UTC each day are available after computation at around 9 UTC the same day. Figure 3a shows the 12-hr time series of the IFS EDR forecast at 240 hPa at the location of the turbulence

encounter (TURB) of flight SQ321, which departed from London on 20 May 2024 at 21:38 UTC. The IFS forecast initialized on 20 May 2024 00 UTC is the latest forecast available prior to departure.

The HRES forecast (Section 3.1) initialized on 20 May 00 UTC shows a maximum in EDR of 0.3 $m^{2/3}$ s^{-1} at 7 UTC followed by low values (<0.1 $m^{2/3}$ s^{-1}) afterward until 12 UTC which is 21:30 local time in Myanmar. The HRES values lie at the upper edge when compared to the other 50 IFS ENS ensemble members at 6 UTC and 7 UTC and close to the median at 8 UTC. The IFS ENS shows an increase of the 90th percentile from about 0.12 $m^{2/3}$ s^{-1} at 6 UTC to about 0.2 $m^{2/3}$ s^{-1} at 8 UTC while the median remains well below 0.1 $m^{2/3}$ s^{-1}. The HRES forecast initialized on 21 May 00 UTC shows a maximum in EDR of 0.2 $m^{2/3}$ s^{-1} at 8 UTC which is close to the 90th percentile of the ENS. However, individual members show values well above 0.2 $m^{2/3}$ s^{-1} at 7 UTC and 8 UTC. The time of the turbulence encounter of flight SQ321 was at 7:49 UTC (Section 2.1). For comparison, maximum EDR measured onboard the research aircraft HALO during the MWT encounter above Iceland was larger than 0.3 $m^{2/3}$ s^{-1}, namely 0.39 $m^{2/3}$ s^{-1} (Bramberger et al., 2020; Wilms et al., 2020). Additional sensitivity runs with the IFS ENS show a narrow distribution with EDR close to 0.05 $m^{2/3}$ s^{-1} when only contributions by the vertical diffusion scheme are taken into account and the terms for convection in Equation 1 are omitted.

The probability for EDR >0.18 $m^{2/3}$ s^{-1} determined from the ENS members of the forecast initialized on 20 May 2024 00 UTC is 12% for 8 UTC at 240 hPa at TURB. When the ENS EDR maxima of ±2 grid points from TURB (±0.2° in latitude and longitude, respectively) are considered, which incorporates the uncertainty of the location of convection among the ENS members, the probability for EDR >0.18 $m^{2/3}$ s^{-1} increases to 36%.

Horizontal maps of EDR at 240 hPa for both HRES forecasts are shown for the time of maximum EDR at TURB, that is 7 UTC for initialization on 20 May 00 UTC (Figure 3b) and 8 UTC for the initialization on 21 May 00 UTC (Figure 3c). Enhanced EDR is mainly found over land and in the ITCZ which corresponds to the occurrence of convection (Section 2.2). It is the convective momentum transport (GWD in Equation 1) that dominated the IFS EDR forecast that day. Both HRES forecasts agree as such that they show the highest risk to encounter severe turbulence along the flight track over Myanmar (Figures 3b and 3c) near the location of the turbulence encounter of flight SQ321 (Section 2). Horizontal maps of the ENS probability for EDR >0.18 $m^{2/3}$ s^{-1} (Figures 3d and 3e) reveal probabilities of 10%–20% over land associated with the predicted occurrence of convection. Locally probabilities of 30%–40% were found for shorter lead time (initialized on 21 May 2024 00 UTC, lead time 8 hr) and the area with enhanced probabilities becomes more focused in a band-like pattern (Figure 3e) which compares well with the convection in the satellite image (Figure 2a).

A vertical cross-section of IFS EDR along the flight track at 7 UTC for the HRES forecast initialized on 20 May 00 UTC (Figure 4a) shows that enhanced EDR (>0.18 $m^{2/3}$ s^{-1}) was predicted in the upper troposphere above 500 hPa and the maximum (>0.3 $m^{2/3}$ s^{-1}) was located close to flight level of SQ321 at 37,000 ft (FL370). Associated convective clouds that could extend above flight level formed in the IFS and are characterized by cloud liquid/ice water content (CLWC, CIWC) of 0.01 g kg^{-1} to 0.1 g kg^{-1}. Developing convection in an earlier stage is found at 16.9°N, 94.6°E (see later times in Figure S4 in Supporting Information S1) and EDR >0.12 $m^{2/3}$ s^{-1} is found at 200 hPa and above, mainly out of clouds (i.e., NCT). Atmospheric stability is reduced between approximately 200 hPa and 120 hPa over land (larger spacing between isentropes in Figure 4a) compared to the parts of the flight track over ocean (smaller spacing between isentropes in Figure 4a).

Although the magnitude of vertical velocity is in general highly underestimated in ECMWF IFS, the updraft which is associated with the convection and CIT is clearly visible in the troposphere around the location of the incident (Figure 4b). At FL370, IFS EDR and vertical velocity maxima close to TURB were 0.25 $m^{2/3}$ s^{-1} and 10 cm s^{-1}, respectively (Figure 4c). The vertical shear of horizontal wind speed in the upper troposphere is strongest over land and above the convective updrafts with an increase from 8 m s^{-1} to 12 m s^{-1} between flight level at 11.5 and 14 km altitude (isotaches in Figure 4b). Even stronger negative (positive) shear is found above the convective updrafts below (above) 15 km altitude. This is where IFS EDR is also >0.18 $m^{2/3}$ s^{-1} (Figure 4a).

4. Discussion and Outlook

The analysis presented above showed that ECMWF IFS was able to predict the occurrence of convection and associated CIT 24 hr in advance when flight SQ321 encountered severe turbulence over Myanmar. The results of

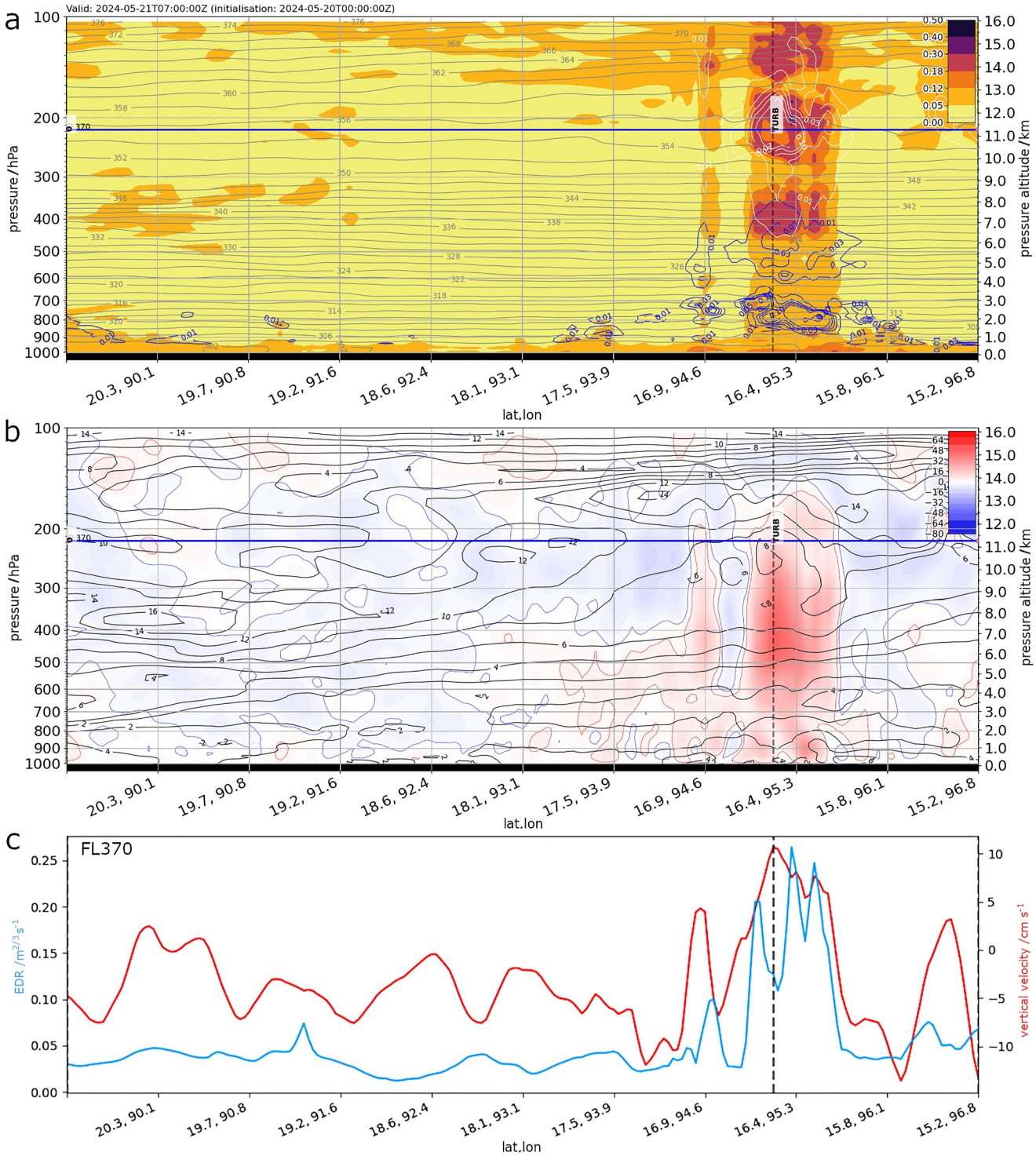

Figure 4. ECMWF IFS forecasts of (a) EDR ($m^{2/3}$ s^{-1}) with cloud liquid/ice water content (blue/white contours, g kg^{-1}) and potential temperature (gray contours, K) and (b) vertical velocity (cm s^{-1}) with horizontal wind speed (black contours, m s^{-1}) along the flight track on 21 May 2024 07 UTC. (c) ECMWF IFS forecasts of EDR (blue) and vertical velocity (red) at flight altitude (FL370) on 21 May 2024 07 UTC. The forecast was initialized on 21 May 2024 00 UTC. Visualization was created with the MSS tool.

the IFS HRES and ENS forecasts revealed the variability and uncertainty of the forecast of the exact time, location, and strength of CIT. For CIT, the IFS relies on the parametrization and representation of the sub-grid scale processes for convection in the IFS. Ingredients for out-of-cloud CIT and NCT were both present in the

IFS fields, that is, strong updrafts, reduced stability in the upper troposphere, enhanced vertical shear of the horizontal wind, and formation of convective clouds. The presence of clouds during the incident was not mentioned in the preliminary report (MOT, 2024) which points to NCT. However, identifying the main ingredient that caused the encountered severe turbulence requires a detailed process study including large eddy simulations of the case. The turbulence could have been caused for example, by the convective updraft itself, small-scale gravity waves, or breaking gravity waves in the shear layer above the convection (Lane et al., 2003).

The variability of convection for the different ensemble members in time and space (Figure 3 and Figure S2 in Supporting Information S1) is related to the initiation and quick development of convection over land in the region (Figure 4 and Figure S4 in Supporting Information S1). The early stage of the convective development influences the derived probabilities of enhanced EDR in IFS ENS forecasts and could distort the impression of the possibility to encounter severe CIT in the area because of resulting probabilities of <20% over Myanmar in the vicinity of the flight track of SQ321.

The turbulence encounter in the area therefore demonstrated that such, apparently low probability must be taken seriously. This is because, as an example, 10 ENS members forecasting an EDR of 0.2 $m^{2/3}$ s^{-1} at a certain location will result in the same probability for EDR >0.18 $m^{2/3}$ s^{-1} as 5 ENS members forecasting an EDR of 0.2 $m^{2/3}$ s^{-1} and 5 ENS members forecasting an EDR of 0.3 $m^{2/3}$ s^{-1}. The risk to encounter severe turbulence is much more likely in the second case. Adjusting the threshold to EDR >0.25 $m^{2/3}$ s^{-1} will result in a probability of 5% for severe turbulence for the second case.

However, one has to keep in mind that despite that one can calculate such probabilities, there is variability in time and space between the ENS members, especially when developing convection is present (Section 3.3). Every member of the ensemble is a possible realization of the future atmospheric state. Therefore, airlines should prepare for turbulence encounters by for example, turning on the fasten seat belt sign, when the IFS ENS EDR forecasts predict individual enhanced and maximum EDR values like for SQ321 (Figure 3a) even though a probability of 5% or 10% for severe turbulence derived from the ENS doesn't sound very likely and alarming.

In the IFS upgrade to cycle 50r1, which is planned for October 2025, the IFS EDR values will be rescaled with a new climatology of aircraft data (for cycle 48r1 the scaling is based on R. D. Sharman and Pearson (2017)) which will further improve the representation of severe turbulence. For the turbulence event of flight SQ321, the new scaling leads to more localized and stronger turbulence in the IFS EDR forecasts (not shown).

The results presented in this study show that the turbulence forecasts available from ECMWF (e.g., on ECMWF, 2024) provide valuable information on convection and CIT, as encountered by flight SQ321, along route prior to departure. As such the forecast could have helped to make the crew aware of potential occurrence of turbulence by convection in the area and to take precautions like switching on the fasten seat belt sign, postponing board service, and request updates by nowcasting services. The implementation of a probabilistic turbulence forecast based on the IFS ensemble was essential and its necessity long known (Lane et al., 2012). However, training is required in order to learn the characteristics of the IFS forecasts for convection and to make proper use of the ENS probabilities for moderate and severe turbulence.

Data Availability Statement

Blog post and ADS-B data are available on https://www.flightradar24.com/blog/1-dead-dozens-injured-in-sq321-turbulence (last access 17 October 2024). ECMWF IFS HRES data are available from the ECMWF archive https://apps.ecmwf.int/archive-catalogue/ (last access 17 October 2024). ECMWF IFS ENS data are provided on zenodo (Bechtold & European Centre for Medium-Range Weather Forecasts, 2024). Satellite brightness temperature data are available for download from Janowiak et al. (2017). The Mission Support System (MSS) tool is available from Bauer et al. (2024).

Acknowledgments
The authors thank Han-Chang Ko from the Department of Atmospheric Sciences, Yonsei University, Seoul, Republic of Korea, for his work on the improvement of the IFS CAT EDR index and the presentation given at ECMWF in May 2024. The authors gratefully acknowledge the use of the MSS flight planning software (Bauer et al., 2022; Rautenhaus et al., 2012). MSS development was partially funded by the Deutsche Forschungsgemeinschaft (DFG, German Research Foundation) project no. UN 311/3-1 and project no. SPP 1294 423229456. The authors thank Andreas Schäfler (DLR) for helpful comments on the manuscript before submission. SG thanks Robert Reichert (LMU/DLR) for assistance with python colormaps. The authors thank Todd Lane and one anonymous reviewer for reviewing this manuscript and providing valuable comments and suggestions. Open Access funding enabled and organized by Projekt DEAL.

References

AusGBM. (2024). Tropical monitoring and outlooks: Madden-Julian Oscillation (MJO). Australian Government Bureau of Meteorology. Retrieved from http://www.bom.gov.au/climate/mjo/#tabs=Monitoring. last access 09 Oct 2024.

Barber, K. A., Deierling, W., Mullendore, G., Kessinger, C., Sharman, R., & Muñoz-Esparza, D. (2019). Properties of convectively induced turbulence over developing oceanic convection. *Monthly Weather Review*, *147*(9), 3429–3444. https://doi.org/10.1175/MWR-D-18-0409.1

Bauer, R., Grooß, J.-U., Ungermann, J., Bär, M., Geldenhuys, M., & Hoffmann, L. (2022). The Mission Support System (MSS v7.0.4) and its use in planning for the SouthTRAC aircraft campaign. *Geoscientific Model Development*, *15*(24), 8983–8997. https://doi.org/10.5194/gmd-15-8983-2022

Bauer, R., Ungermann, J., Grooß, J.-U., Rolf, C., Rißе, M., & Rautenhaus, M. (2024). Mission Support System software [software]. *Zenodo*. https://doi.org/10.5281/zenodo.12656765

Bechtold, P., & European Centre for Medium-Range Weather Forecasts. (2024). IFS CAT EDR ensemble data [Dataset]. *Zenodo*. https://doi.org/10.5281/zenodo.13148844

Bechtold, P., Bramberger, M., Dörnbrack, A., Isaksen, L., & Leutbecher, M. (2021). Experimenting with a clear air turbulence (CAT) index from the IFS (No. 874). *ECMWF*. https://doi.org/10.21957/4l34tqljm

Bramberger, M., Dörnbrack, A., Wilms, H., Ewald, F., & Sharman, R. (2020). Mountain-wave turbulence encounter of the research aircraft HALO above Iceland. *Journal of Applied Meteorology and Climatology*, *59*(3), 567–588. https://doi.org/10.1175/JAMC-D-19-0079.1

Dörnbrack, A., Bechtold, P., & Schumann, U. (2022). High-resolution aircraft observations of turbulence and waves in the free atmosphere and comparison with global model predictions. *Journal of Geophysical Research: Atmospheres*, *127*(16), e2022JD036654. https://doi.org/10.1029/2022JD036654

ECMWF. (2020). 43r1 new parameters: Height of convective cloud top. Retrieved from https://confluence.ecmwf.int/pages/viewpage.action?pageId=65221941. last access 30 Sept 2024.

ECMWF. (2023a). IFS documentation CY48R1 - Part IV: Physical processes. *IFS Documentation CY48R1*(4). https://doi.org/10.21957/02054f0fbf

ECMWF. (2023b). IFS documentation CY48R1 - Part V: Ensemble prediction system. *IFS Documentation CY48R1*(5). https://doi.org/10.21957/e529074162

ECMWF. (2024). ECMWF charts. Retrieved from https://charts.ecmwf.int/?facets=&query=turbulence. last access 11 Nov 2024.

Eichenbaum, H. (2003). Historical overview of turbulence accidents and case study analysis. *MCR Federal Inc. Rep. Br-M021/080–1*, 82.

FAA. (2017). *Safety of flight. Aeronautical information manual: Official guide to basic flight information and ATC procedures*. U.S. Dept. of Transportation.

Janowiak, J., Joyce, B., & Xie, P. (2017). NCEP/CPC L3 half hourly 4km global (60S - 60N) merged IR V1 Andrey Savtchenko, Greenbelt, MD, Goddard Earth Sciences data and information services center (GES DISC) [Dataset]. https://doi.org/10.5067/P4HZB9N27EKU. last access 1 August 2024.

Kim, J.-H., & Chun, H.-Y. (2012a). Development of the Korean aviation turbulence guidance (KTG) system using the operational unified model (UM) of the Korea meteorological administration (KMA) and pilot reports (PIREPs). *Journal of the Korean Society for Aviation and Aeronautics*, *20*(4), 76–83. https://doi.org/10.12985/ksaa.2012.20.4.076

Kim, J.-H., & Chun, H.-Y. (2012b). A numerical simulation of convectively induced turbulence above deep convection. *Journal of Applied Meteorology and Climatology*, *51*(6), 1180–1200. https://doi.org/10.1175/jamc-d-11-0140.1

Kim, S.-H., Chun, H.-Y., Lee, D.-B., Kim, J.-H., & Sharman, R. D. (2021). Improving numerical weather prediction–based near-cloud aviation turbulence forecasts by diagnosing convective gravity wave breaking. *Weather and Forecasting*, *36*(5), 1735–1757. https://doi.org/10.1175/WAF-D-20-0213.1

Kim, S.-H., Kim, J.-H., Chun, H.-Y., & Sharman, R. D. (2023). Global response of upper-level aviation turbulence from various sources to climate change. *npj Climate and Atmospheric Science*, *6*(1), 92. https://doi.org/10.1038/s41612-023-00421-3

Lane, T. P., Sharman, R. D., Clark, T. L., & Hsu, H.-M. (2003). An investigation of turbulence generation mechanisms above deep convection. *Journal of the Atmospheric Sciences*, *60*(10), 1297–1321. https://doi.org/10.1175/1520-0469(2003)60⟨1297:AIOTGM⟩2.0.CO;2

Lane, T. P., Sharman, R. D., Trier, S. B., Fovell, R. G., & Williams, J. K. (2012). Recent advances in the understanding of near-cloud turbulence. *Bulletin of the American Meteorological Society*, *93*(4), 499–515. https://doi.org/10.1175/BAMS-D-11-00062.1

MOT. (2024). Transport safety investigation Bureau preliminary investigation findings of incident involving SQ321. Retrieved from https://www.mot.gov.sg/news/Details/transport-safety-investigation-bureau-preliminary-investigation-findings-of-incident-involving-sq321. last access 1 August 2024.

Prosser, M. C., Williams, P. D., Marlton, G. J., & Harrison, R. G. (2023). Evidence for large increases in clear-air turbulence over the past four decades. *Geophysical Research Letters*, *50*(11), e2023GL103814. https://doi.org/10.1029/2023GL103814

Rapp, M., Kaifler, B., Dörnbrack, A., Gisinger, S., Mixa, T., Reichert, R., et al. (2021). SOUTHTRAC-GW: Gravity waves meet sudden stratospheric warming. *Bulletin of the American Meteorological Society*, *102*(12), 1158–1166. https://doi.org/10.1175/BAMS-D-20-0034.A

Rautenhaus, M., Bauer, G., & Dörnbrack, A. (2012). A web service based tool to plan atmospheric research flights. *Geoscientific Model Development*, *5*(1), 55–71. https://doi.org/10.5194/gmd-5-55-2012

Sharman, R., Tebaldi, C., Wiener, G., & Wolff, J. (2006). An integrated approach to mid- and upper-level turbulence forecasting. *Weather and Forecasting*, *21*(3), 268–287. https://doi.org/10.1175/WAF924.1

Sharman, R. D., Cornman, L. B., Meymaris, G., Pearson, J., & Farrar, T. (2014). Description and derived climatologies of automated in situ eddy-dissipation-rate reports of atmospheric turbulence. *Journal of Applied Meteorology and Climatology*, *53*(6), 1416–1432. https://doi.org/10.1175/JAMC-D-13-0329.1

Sharman, R. D., & Pearson, J. M. (2017). Prediction of energy dissipation rates for aviation turbulence. Part I: Forecasting nonconvective turbulence. *Journal of Applied Meteorology and Climatology*, *56*(2), 317–337. https://doi.org/10.1175/JAMC-D-16-0205.1

Sharman, R. D., Trier, S. B., Lane, T. P., & Doyle, J. D. (2012). Sources and dynamics of turbulence in the upper troposphere and lower stratosphere: A review. *Geophysical Research Letters*, *39*(12), L12803. https://doi.org/10.1029/2012GL051996

Wheeler, M. C., & Hendon, H. H. (2004). An all-season real-time multivariate MJO index: Development of an index for monitoring and prediction. *Monthly Weather Review*, *132*(8), 1917–1932. https://doi.org/10.1175/1520-0493(2004)132<1917:aarmmi>2.0.co;2

Williams, P. D. (2017). Increased light, moderate, and severe clear-air turbulence in response to climate change. *Advances in Atmospheric Sciences*, *34*(5), 576–586. https://doi.org/10.1007/s00376-017-6268-2

Wilms, H., Bramberger, M., & Dörnbrack, A. (2020). Observation and simulation of mountain wave turbulence above Iceland: Turbulence intensification due to wave interference. *Quarterly Journal of the Royal Meteorological Society*, *146*(732), 3326–3346. https://doi.org/10.1002/qj.3848